Acta Biomaterialia 17 (2015) 201–209

Contents lists available at ScienceDirect

Acta Biomaterialia

journal homepage: www.elsevier.com/locate/actabiomat

Near-infrared light remote-controlled intracellular anti-cancer drug delivery using thermo/pH sensitive nanovehicle

Yanping Qin [a,b], Jun Chen [b,*], Ying Bi [a,b], Xiaohan Xu [b], Hui Zhou [a,b], Jimin Gao [a,*], Yi Hu [b,*], Yuliang Zhao [b], Zhifang Chai [b,c]

[a] School of Laboratory Medicine and Life Science, Wenzhou Medical University, Wenzhou 325035, Zhejiang Province, China
[b] Key Laboratory for Biomedical Effects of Nanomaterials and Nanosafety, Institute of High Energy Physics, Chinese Academy of Sciences, Beijing 100049, China
[c] School of Radiological and Interdisciplinary Sciences, Soochow University, Suzhou 215123, China

ARTICLE INFO

Article history:
Received 11 August 2014
Received in revised form 11 November 2014
Accepted 20 January 2015
Available online 30 January 2015

Keywords:
Near-infrared light
Photothermal effect
Carbon nanotube
pH/temperature sensitivity
Intracellular drug delivery

ABSTRACT

Stimuli-responsive drug delivery systems have been developed to enhance the tumor-targeting drug transportation and minimize the severe side effects along with the chemotherapy. In this study, a near-infrared (NIR) light triggered drug delivery system was developed based on the amphiphilic chitosan derivative-coated single-wall carbon nanotubes (CNT) encapsulated in the thermo/pH sensitive nanogel (CS/PNIPAAm@CNT). The PEG diacrylate (Mw = 250 Da) was applied in the present work to tune the nanoparticles with the phase transition temperature at ~38 °C, which was an attempt to match the prerequisite for the *in vivo* applications. Owing to the π–π stacking, hydrophobic interaction and the opportunity of Schiff-base formation between chitosan and doxorubicin (DOX), the nanoparticles possessed a relative high drug loading capacity (~43%). The DOX loaded CS/PNIPAAm@CNT released DOX faster at 40 °C than at 25 °C, meanwhile faster at pH 5.0 in comparison with that at pH 7.4. Moreover, the rapid and repetitive release of DOX was observed when the DOX-loaded CS/PNIPAAm@CNT was irradiated under NIR light. Furthermore, DOX-loaded CS/PNIPAAm@CNT upon NIR irradiation showed significantly greater cytotoxicity in HeLa cells owing to NIR-triggered increase in temperature and enhanced DOX release. Confocal laser scanning microscopy (CLSM) was utilized to demonstrate the enhanced cell uptake of the as prepared nanoparticles and the faster drug release under the NIR irradiation and lower pH. All the results suggest that multifunctional DOX-loaded CS/PNIPAAm@CNT nanocomposite is a promising therapeutic nanocarrier for intracellular drug delivery with great potential for targeted cancer therapy.

1. Introduction

Stimuli-responsive drug delivery systems have recently been widely explored in attempt to address the problems in chemotherapy, such as the multidrug resistance, severe side effects, and metastasis [1–9]. Currently, more and more investigations focus on the noninvasive external stimuli responsive drug delivery and therapy because they allow remote, repetitive, and reliable tuning of drug release based on demand. Among them, near infrared (NIR) light (650–900 nm) triggered drug release systems can efficiently absorb NIR light and convert it into heat which drives the drug release from a thermosensitive carrier [10–13]. So far, NIR-based thermosensitive drug delivery systems have shown great potential in targeted drug delivery due to their effective drug accumulation in local regions, good penetration through tissue and minimal tissue damages [11,14–18].

Carbon nanotube (CNT) is one of the ideal candidates to absorb the NIR light and convert it to heat in high efficiency, which exhibits great potential for photothermal therapy *in vitro* and *in vivo* [10,19–21]. It is a promising nanoscaled vector which has been demonstrated to efficiently deliver water-insoluble anticancer drugs, proteins, genetic therapeutics, and bioimaging agents into cells. Nevertheless, several distinct shortcomings including poor solubility and surface functionalization seriously hinder its biomedical applications. To overcome these impediments, the development of composite nanomaterials utilizing biocompatible polymeric materials and CNT becomes a promising solution [22–25].

In the present work, we took the advantage of the high photothermal sensitivity of CNT as the NIR stimulus antenna and a thermo/pH sensitive nanogel as the carrier for NIR-remoting and acidic pH accelerating release of anti-cancer drugs. Poly(N-isopropylacrylamide) (PNIPAAm) was selected as the thermo responsive

* Corresponding authors. Fax: +86 10 88236730 (J. Chen), +86 577 86689748 (J. Gao), +86 10 88236730 (Y. Hu).
E-mail addresses: chenjun@ihep.ac.cn (J. Chen), jimingao64@163.com (J. Gao), huyi@ihep.ac.cn (Y. Hu).

http://dx.doi.org/10.1016/j.actbio.2015.01.026
1742-7061/

material in this design, which undergoes a reversible discontinuous phase transition in water, changing from hydrophilicity (swelling) to hydrophobicity (shrinking) in response to a temperature change [26]. Chitosan (CS) functionalized with hydrophobic alkyl chains in the side chains with controllable ratios was synthesized to finely disperse the CNT in the aqueous media [27]. Doxorubicin (DOX) was loaded into CS/PNIPAAm@CNT nanomaterials, and the formation of Schiff base bonds between the primary amino groups of chitosan and the ketone groups of DOX endowed the drug carrier system with pH sensitivity. pH sensitivity, which could be achieved through hydrazone bonds [28–30], Schiff base [31] or titrable amine groups [32,33], is the most frequently employed external stimulus to trigger the drug release. The morphology of nanoparticles, hydrodynamic diameter, thermo/pH sensitivities and cytotoxicity of CS/PNIPAAm@CNT nanoparticles were characterized. After the evaluation of the drug loading capacity and efficiency, thermo/pH sensitive release and NIR-light-triggered drug release from CS/PNIPAAm@CNT were measured *in vitro*. Moreover the uptake of DOX loaded CS/PNIPAAm@CNT and intracellular drug distributions upon various stimuli were investigated in HeLa cells using confocal laser scanning microscopy. The NIR light-mediated cancer chemotherapy is expected to become a novel tumor-targeting strategy with facile spatio-temporal control to enhance the anticancer treatment outcomes.

2. Materials and methods

2.1. Materials

All chemicals were purchased from Sigma–Aldrich China Ltd. and used without further purification unless otherwise noted. The CNTs were purchased from Chengdu Organic Chemicals Co., Ltd., with a diameter of 1–2 nm and a length of 1–3 μm. The 3-(4,5-dimethyl thiazolyl-2)-2, 5-diphenyl tetrazolium bromide (MTT), 4′,6-diamidino-2-phenylindole (DAPI) and BODIPY® FL phalloidin were purchased from Invitrogen Inc. Dialysis membrane (Cutoff = 3.5 kDa and 7 kDa MWCO), 0.45 μm Millipore Millex Syringe Filters were purchased from Sigma–Aldrich China Ltd. Carbon coated copper grids were purchased from Xinxing Braim Tech Co., Ltd. (Beijing, China). Cervical cancer cells (HeLa) were kindly gifted by Peking Union Medical College.

2.2. Characterizations of nanoparticles

The UV absorbance was recorded with a Varian Cary-50 UV–vis spectrophotometer. Images of the micelles were recorded by a Hitachi S-4800 scanning electron microscope (SEM) and recorded using an AMT digital camera. Hydrodynamic diameters (Dh) and size distributions were determined by Malvern Zetasizer Nano-S dynamic light scattering (DLS) (Malvern Instruments Ltd. Worcestershire, UK). Measurements were conducted at predetermined temperature and pH values.

2.3. Synthesis of chitosan-g-oleic acid copolymer (CS-OA)

Oleic acid (0.14 mmol, 40.0 mg), N-(3-dimethylaminopropyl)-N′-ethylcarbodiimide hydrochloride (EDC, 0.14 mmol, 26.8 mg) and N-hydroxysuccinimide (NHS, 0.14 mmol, 16.1 mg) were dissolved in 10 ml of N,N-dimethylformamide (DMF) and stirred at room temperature for 1 h. Then the mixture was added into 100 ml 0.25% w/t chitosan aqueous solution, and the mixture was stirred overnight at room temperature. The product was then precipitated in large excess of THF. The precipitation was collected and subsequently dialyzed against distilled water for 3 days. The white solid was collected after the lyophilization.

2.4. Pretreatment of single-wall carbon nanotubes

The pristine CNTs were prepared with a diameter of 1–2 nm and a length of 1–3 μm. The cutting and acidification process of pristine CNTs were conducted as follows: 100 mg CNTs were dispersed into 80 ml mixture of concentrated sulfuric acid and nitric acid (v/v, 3:1) and sonicated continuously for 24 h at 0 °C followed by centrifugation at 10,000 rpm for 10 min [25]. Subsequently, the supernatant was centrifuged at 14,000 rpm for 30 min and then the sediment was neutralized by 1 M Na_2CO_3 followed by the extensive dialysis. The truncated CNTs were obtained via lyophilization.

2.5. Preparation of CS-OA@CNT nanomaterials

CS-OA@CNT was prepared as follows: The truncated CNTs were added into 10 mg/ml sodium cholate, followed by sonication for 24 h at 0 °C and centrifuging for 30 min at 10,000 rpm. The supernatant was added into 100 ml 0.25% w/t CS-OA copolymer solution and dialyzed against distilled water for 72 h. The gray powder was obtained via lyophilization.

2.6. Preparation of CS/PNIPAAm@CNT nanoparticles

CS/PNIPAAm@CNT nanoparticles were prepared according to a previous report with modifications [34]: the aqueous solution of 1.0 g NIPAAm and 20 mg crosslinkers, including poly(ethylene glycol) diacrylate with molecular weight of 250 g/mol (PEGDA250) and 700 g/mol (PEGDA700), N,N′-methylenebisacrylamide (MBA), were added dropwise to 100 ml 0.25% w/t CS-OA@CNT solution at 70 °C and then stirred at 3000 rpm for 30 min with air-purging of Ar. 10 ml of 1 mg/ml initiator, ammonium persulfate aqueous solution, was added dropwise into above mentioned solution, which was then stirred for 3 h in dark at 70 °C to form the nanoscaled interpenetration network matrix. The whole process was protected by Ar [35]. The dispersed product was transferred to a dialysis bag (molecular weight cut-off = 7000 Da) and dialyzed against distilled water for 3 d to remove impurities and by-products. The powder of CS/PNIPAAm@CNT nanoparticles was obtained by lyophilization.

2.7. Preparation of DOX-loaded CS/PNIPAAm@CNT nanoparticles

DOX-loaded CS/PNIPAAm@CNT nanoparticles were prepared as follows: briefly, different amounts of DOX hydrochloride were dissolved in 2 ml DMSO, which was stirred with 1.5 equivalent of triethylamine, followed by addition of 20 mg of freeze-dried CS/PNIPAAm@CNT nanoparticles. The mixture was allowed to be sonicated for 30 min and stirred for 6 h at room temperature in dark. The mixture was transferred to a dialysis bag (molecular weight cut-off = 7 kDa) and dialyzed for 24 h to remove free DOX and by-products. Finally, the DOX-loaded CS/PNIPAAm@CNT nanoparticles were lyophilized to obtain a red powder. Encapsulation efficiency and drug-loading capacity of DOX-loaded CS/PNIPAAm@CNT nanoparticles were quantified by dissolving nanoparticles in DMSO and testing its absorbance at 480 nm by using UV–vis spectroscopy. A standard curve was acquired with DOX/DMSO solutions containing different concentrations of DOX. Encapsulation efficiency and drug-loading capacity were calculated according to the following equations:

$$\text{Drug encapsulation efficiency as a percentage} = (\text{weight of loaded drug})/(\text{weight of feeding drug}) \times 100\%$$

$$\text{Drug loading capacity as a percentage} = (\text{weight of loaded drug})/(\text{weight of nanovectors} + \text{weight of loaded drug}) \times 100\%$$

2.8. In vitro DOX release from DOX-loaded CS/PNIPAAm@CNT nanoparticles

The temperature-sensitive and pH-sensitive drug release profiles were measured using a dynamic dialysis method. The dispersed solution of 0.8 mg DOX-loaded nanoparticles was added into a dialysis bag (Mw cut-off = 3.5 KDa). The bag was placed in 50 ml phosphate-buffered saline (PBS, 0.1 M, pH = 7.4) in a vial at room temperature or 37 °C under stirring at 200 rpm. At predetermined intervals, 10 ml was withdrawn from the vial to measure DOX absorbance at 480 nm, and then 10 ml of fresh PBS was added to maintain 50 ml buffer solution in the vial. The concentrations of DOX were calculated from a standard curve of DOX absorbance.

In vitro pH-sensitive drug release profiles were obtained using the same dynamic dialysis method as mentioned above [36]. Experiments were conducted at pH = 5.0 (acetate buffer) and pH = 7.4 (PBS buffer) at 37 °C, respectively.

To test the NIR triggered DOX release, two groups of samples were prepared in the release profile, and the concentration of DOX was kept the same as 0.1 mg/ml in both samples. Sample 1 containing 2 ml DOX-CS/PNIPAAm@CNT nanoparticle suspension was irradiated with the 808 nm NIR light (1 W/cm^2, 1 cm^2 faculous region) over a period of 3 min. Sample 2 was treated without NIR. Two samples were placed in two dialysis bags (Mw cut-off = 3.5 kDa), respectively. The dialysis bags were placed in 10 ml PBS (0.1 M, pH = 7.4) in a vial at 37 °C and stirred at 200 rpm. At predetermined time, 2 ml solution was withdrawn from the vial to measure DOX absorbance at 480 nm, and 2 ml of fresh PBS was added to maintain the volume in the vial. The concentrations of DOX were calculated from a standard curve of DOX absorbance.

2.9. Cytotoxicity of DOX-loaded CS/PNIPAAm@CNT micelles

HeLa cell line was used to investigate cell growth inhibition of DOX-loaded nanoparticles. HeLa cells were cultured with Dulbecco's Modified Eagle's Medium (DMEM, GIBCO) supplemented with 10% fetal bovine serum (FBS, GIBCO), 1.0×10^5 U/l penicillin (Sigma) and 100 mg/l streptomycin (Sigma) at 37 °C in 5% CO_2.

The cytotoxicity of the nanoparticles loaded with DOX was determined using a MTT cell proliferation kit (Biotium Inc.). HeLa cells were seeded into a 96-well tissue culture plate at a density of 8000 cells per well and were incubated at 37 °C with 5% CO_2. The growth medium was replaced with fresh DMEM after 24 h. Then the DOX-loaded CS/PNIPAAm@CNT or control samples (free DOX and blank nanoparticles solutions) were added into wells (six wells per sample). Some groups of cells were then irradiated with NIR laser (808 nm) from the top. Cells were cultured for another 24 h or 48 h, then 10 μl MTT solution was added into each well and incubated for another 4 h. The medium was removed and 200 μl DMSO was added into each well to dissolve the formazan by pipetting in and out several times. The absorbance of each well was measured using an ELISA plate reader at a test wavelength of 570 nm and a reference wavelength of 630 nm. The cell growth inhibition of samples was calculated as:

$$\text{Cell inhibition}(\%) = \frac{I_{\text{control}} - I_{\text{sample}}}{I_{\text{control}}} \times 100\%$$

where I_{sample} and I_{control} represent the intensity determined for cells treated with different samples and for control cells (untreated), respectively.

2.10. Cell uptake and intracellular drug distribution of DOX-loaded CS/PNIPAAm@CNT nanoparticles

Confocal laser scanning microscopy (CLSM) was utilized to investigate the cellular uptake and drug distribution of DOX by incubating the HeLa cells with DOX-loaded nanoparticles or free DOX for 15 min, 2 h and 24 h. Firstly, the HeLa cells were incubated in the culture dish which was covered by a glass slip at a density of 10,000 cells/dish (diameter = 3.5 cm) and cultured for 24 h. After predetermined incubation time with the DOX or DOX loaded nanoparticles, PBS was used to wash the cells and 4% paraformaldehyde/PBS solution was added to fix the cells. After 15 min incubation, the cover slip was washed with PBS. The enhanced permeabilization was accomplished by incubation with 0.1% Triton X-100/PBS for 10 min followed by rinsing with PBS buffer for three times. The cells were incubated in 0.1 μM BODIPY® FL phalloidin/1% (w/v) BSA solution for 20 min and then rinsed with PBS three times. The visualization of the cell nuclei was accomplished by incubation in 10 μg/ml DAPI for 10 min and then rinsed with PBS buffer for three times. At last, the cover slip was fixed on a microscope slide and observed by CLSM.

2.11. Statistical analysis

All of the data are presented as the mean value ± standard deviation (SD) and all experiments were performed with at least 3 independent repeats. Differences between groups were examined using Student's *t*-test between two groups. A value of $P < 0.05$ was considered statistically significant.

3. Results and discussion

3.1. The preparation and characterization of DOX-loaded CS/PNIPAAm@CNT nanoparticles

In this study, we devised a NIR light remote triggered and pH sensitive drug delivery system based on amphiphilic chitosan derivatives coated single-wall CNT and PNIPAAm nanogels as shown in Scheme 1. We hypothesized that the CNT embedded in the nanogels could act as an antenna to receive the NIR light and convert it to heat, which will induce shrinkage of the PNIPAAm and boost the release DOX from the nanogels. Simultaneously, the endosomal acidic pH will boost the degradation of the Schiff base bonds and the release the DOX from the interior of gel matrix.

The DOX was encapsulated into CS/PNIPAAm@CNT by a solvent replacement procedure. The DMSO was exploited in this step as a good solvent for nanogels and drugs, which made the nanogel swollen and enhanced the physical diffusion of drug in the nanoparticles. Subsequently, the DOX may possibly undergo three distinct major interactions with CS/PNIPAAm@CNT to be entrapped inside the gel matrix. One was resulted from the hydrophobic interaction and π–π interaction existing between dehydrochloride DOX molecules and CNT. These interactions of poor-soluble molecules and CNTs have gained extensive interests in previous studies [37,38]. The second interaction was the formation of Schiff base bonds derived from the primary amino groups in the chitosan and the ketone groups in the DOX molecules. This formation of acid-labile covalent conjugation by primary amino groups in chitosan and ketone groups in DOX would enhance the DOX immobilization into the as prepared nanoparticles and endow the nanoparticles with pH-sensitive property. The third interaction was the physical entrapment of DOX in the nanogel matrix. The interpenetration structure of the nanogels matrix constructed by chitosan and PNIPAAm would facilitate encapsulation of DOX.

The preparation of the nanomaterials was started from synthesis of chitosan-*graft*-oleic acid. The chemical compositions of pristine chitosan, chitosan-*graft*-oleic acid, PNIPAAm, CNTs, free DOX, and DOX-loaded CS/PNIPAAm@CNT nanoparticles were characterized by FT-IR spectrometry as shown in Fig. 1. For the FT-IR curve of chitosan, the peak at ~3400 cm^{-1} corresponded to the

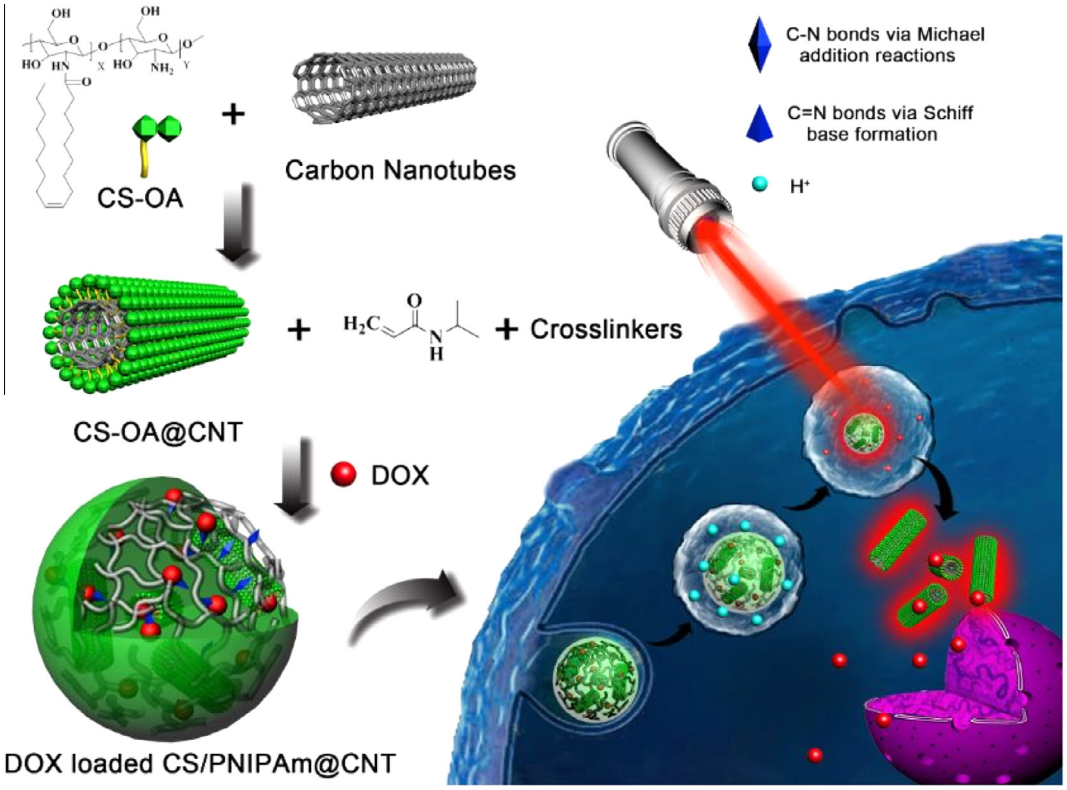

Scheme 1. Schematic illustration of DOX/CS/PNIPAAm@CNT nanoparticles and the drug release in response to the pH decrease and the temperature increase induced by the NIR light irradiation.

—OH groups in the backbone of the polysaccharide. The peak of 1390 cm^{-1} was associated with C—O stretching of the primary alcoholic groups in chitosan. This peak was also observed in the DOX-CS/PNIPAAm@CNT nanoparticles. The chitosan-*g*-oleic acid had a similar FT-IR absorbance as to the pristine chitosan, while the most significant difference existed in the peaks around 2900 cm^{-1} which was attributed to C—H asymmetric stretching of the alkyl chains in chitosan-*g*-oleic acid. Two peaks at 1660 and 1550 cm^{-1} can be observed in both DOX-CS/PNIPAAm@CNT nanoparticles and PNIPAAm. These absorbance peaks were attributed to the C=O stretching and the secondary amide N—H deformation vibration of PNIPAAm. The results suggested that the DOX-CS/PNIPAAm@CNT nanoparticles consisted of chitosan derivatives and PNIPAAM. The O—H (3435 cm^{-1}) and C=O (1625 cm^{-1}) from —COOH indicated the successful oxidization of CNTs. For free DOX, the peak at ~1720 cm^{-1} was attributed to the C=O stretching movement adjacent to the phenyl groups. Together with the bands at 3448 cm^{-1} and 1624 cm^{-1} (attributed to the O—H and N—H

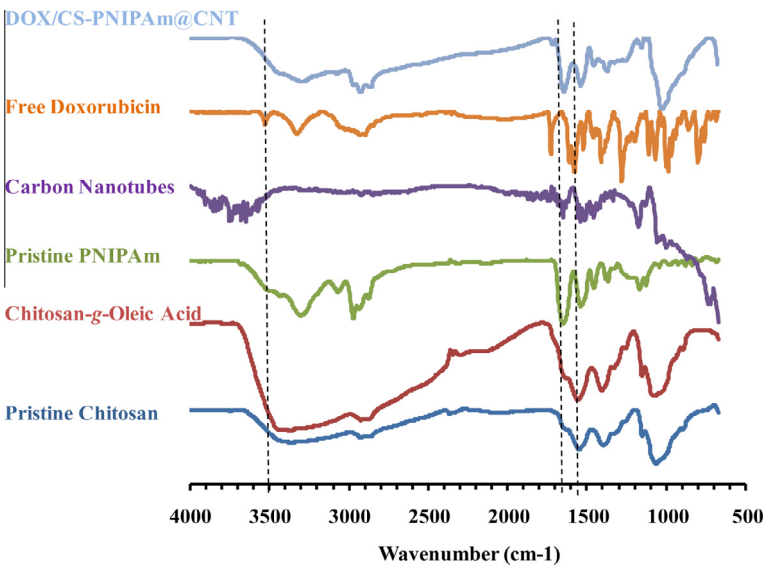

Fig. 1. FT-IR characterization of DOX-loaded CS/PNIPAAm@CNT, CNT, PNIPAAm, Chitosan, CS-OA copolymer and free doxorubicin.

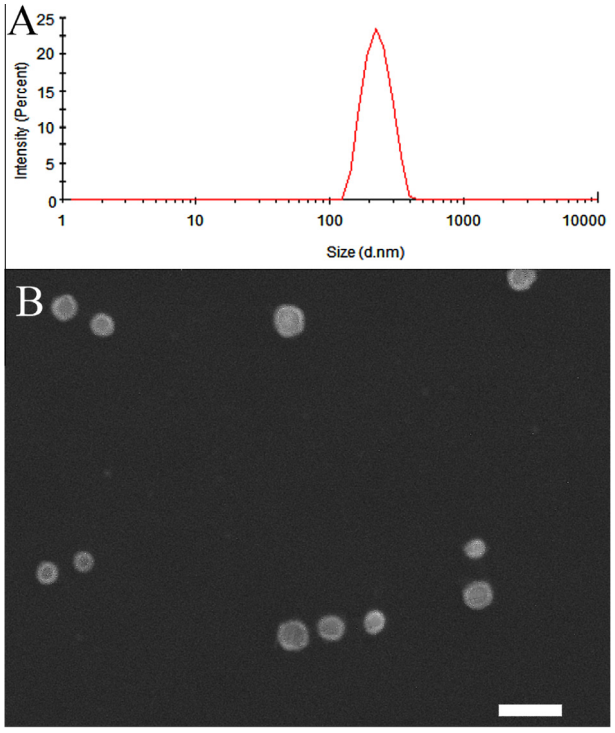

Fig. 2. (A) Hydrodynamic diameter of CS-OA@CNT. (B) SEM image of DOX-loaded CS/PNIPAAm@CNT nanoparticles. Scale bar: 1 μm.

group on DOX, respectively), these peaks can also be observed in the DOX/CS/PNIPAAm@CNT nanoparticles, which suggested the successful encapsulation of drugs.

The size of chitosan-oleic acid coated CNTs was evaluated by the dynamic light scattering. As shown in Fig. 2A, the diameter of surface coated truncated CNTs was ~240 nm with a moderate size distribution. Furthermore, the SEM image of the CS/PNIPAAm@CNT nanoparticles confirmed that the diameter was averagely 300 nm and the size distribution of the nanoparticles was narrow. The prepared particles showed a spherical morphology and homogeneous size.

The sensitivity of the nanoparticles toward the environmental temperature is essential for their application in controlled release in this study. The thermal-sensitivity of nanoparticles was investigated by DLS. The particle size changed with the variation of temperature value as shown in Fig. 3. At 25 °C, the hydrodynamic diameter of CS/PNIPAAm@CNT crosslinked by MBA (MBA-CS/PNIPAAm@CNT) was around 300 nm with monodispersity which was consistent with the data observed by SEM, while the hydrodynamic diameter of CS/PNIPAAm@CNT crosslinked by PEGDA 250 (PEGDA250-CS/PNIPAAm@CNT) was around 240 nm. The lower critical solution temperature (LCST) of MBA-CS/PNIPAAm@CNT was exhibited starting from ~32 °C. When the temperature was elevated to 37 °C, the hydrodynamic diameter of MBA-CS/PNIPAAm@CNT was changed to about 240 nm. The diameter of the particles was prone to decrease due to dehydration of polymer chains of PNIPAAm and the collapse of the hydrophilic segments when temperature is above its phase transition temperature (about 32 °C) [26]. But when the as prepared nanoparticles were crosslinked by more hydrophilic crosslinker PEGDA, the LCST range of PEGDA250-CS/PNIPAAm@CNT was shifted to ~38–39 °C. When the hydrophilicity of crosslinker was further increased, the PEGDA700-CS/PNIPAAm@CNT had no distinct LCST, which indicated that the dehydration of PNIPAAm was unable to affect the hydrophilicity of nanoparticles. This phenomenon was in agreement with the previous studies of PNIPAAm-associated LCST [39]. And this elevation of LCST was essential to the application of our nanoparticles for *in vivo* drug delivery. In turn, the CS/PNIPAAm@CNT crosslinked by PEGDA250 was used in the subsequent research.

3.2. In vitro release studies of drug-loaded CS/PNIPAAm@CNT nanoparticles

The cytosol of healthy tissues and blood has the pH value of about 7.4, and the pH values in endosomes and lysosomes ranged from 6.5 to 5.0 [28]. Therefore, a myriad of pH responsive nanomaterials have been developed as intracellular drug nanovectors [28,40,41]. The formation of Schiff base bonds is one of the general designs. In this research, the pH-dependent property of Schiff-base conjugation was employed for designing of a pH sensitive CS/PNIPAAm@CNT nanocomposites. Meanwhile, the innate pH sensitivity of DOX molecules was another major factor to accelerate the DOX release from the nanoparticle under acidic pH environment. In addition to the pH sensitive property, the thermal-dependent characteristic of PNIPAAm was also harnessed to endow the nanovectors with temperature sensitive property.

For drug delivery systems, the high drug loading capacity is one of the important evaluation criteria. In this study, it was found that the DOX-loading efficiency of prepared nanoparticles was ~90%, and DOX loading capacity was ~43.3 wt%, which is significantly higher compared with previous reported nanogels drug delivery systems [14,42,43]. For example, Zhang et al. fabricated a nanocomposite by further coating AuNR@SiO2 with a thermo- and

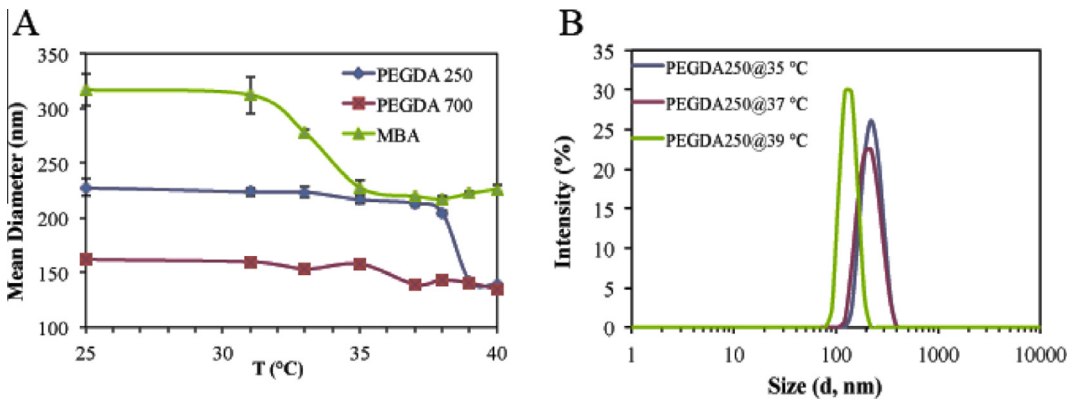

Fig. 3. (A) Temperature dependent size change of three kinds of CS/PNIPAAm@CNT prepared by the crosslinkers of PEGDA 250, PEGDA700 and MBA, respectively. (B) Hydrodynamic diameter change of CS/PNIPAAm@CNT prepared by the crosslinkers of PEGDA 250 monitored by the DLS at the different temperature.

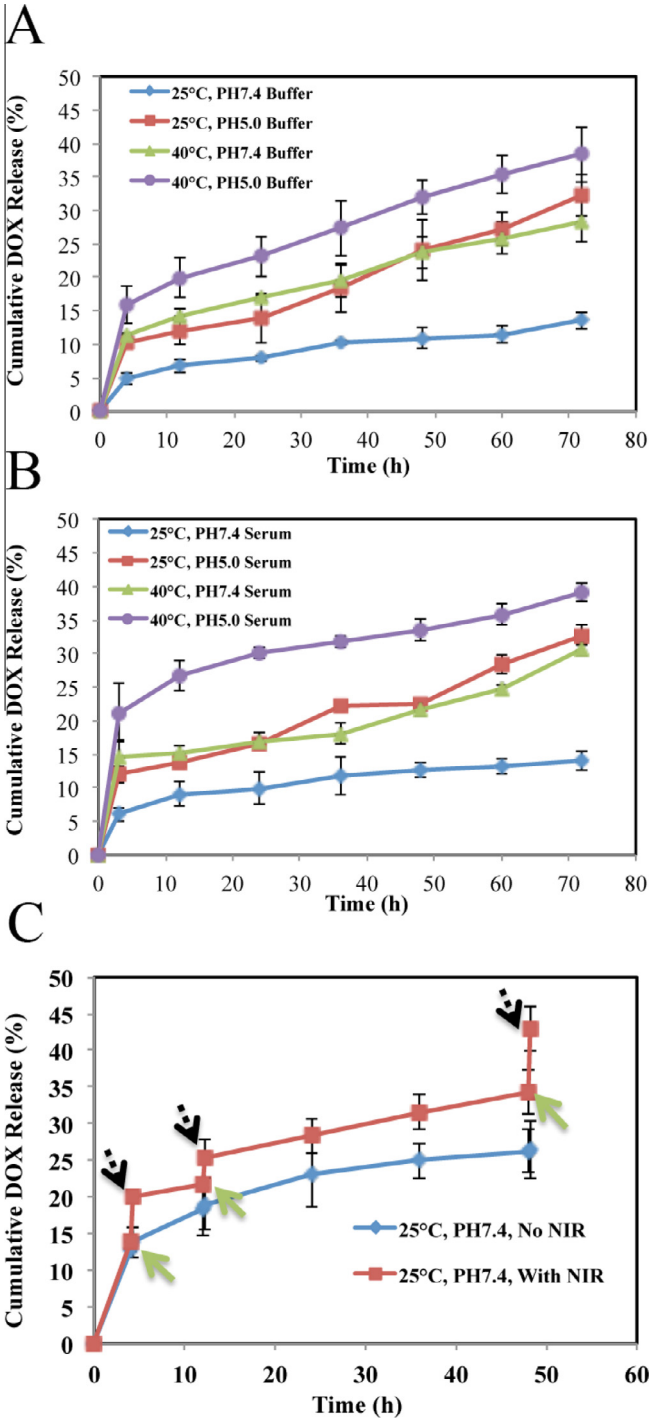

Fig. 4. (A) Cumulative DOX release profile of DOX-loaded CS/PNIPAAm@CNT nanoparticles at different temperatures or pH values. (B) Cumulative DOX release profile of DOX-loaded CS/PNIPAAm@CNT nanoparticles in serum at different temperatures or pH values. (C) The cumulative DOX release from DOX-loaded CS/PNIPAAm@CNT nanoparticles upon NIR irradiation. The green arrows point at the time points when switching on the laser. The black arrows point at the time points when switching off the laser.

pH-responsive polymer shell, poly(N-isopropylacrylamide-co-acrylic acid) and explored its *in vivo* applications [14]. DOX was loaded into the nanocomposite through electrostatic interactions, with a loading content up to 24%, which is significantly lower than ~43 wt% drug loading content in CS/PNIPAAm@CNT nanoparticles.

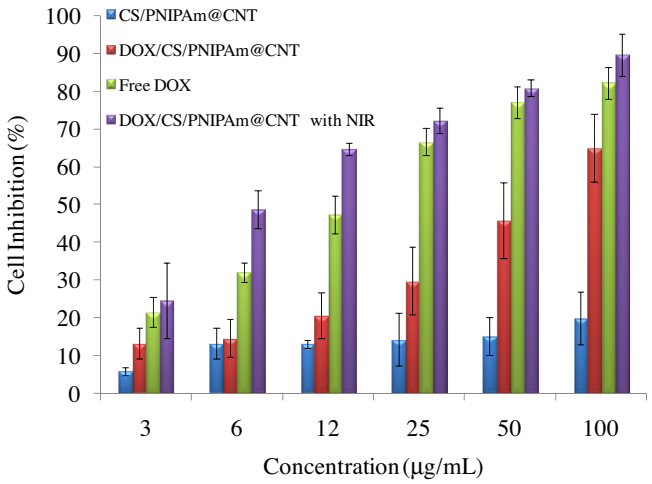

Fig. 5. Cell growth inhibition rate of free DOX, CS/PNIPAAm@CNT nanoparticles, DOX-loaded CS/PNIPAAm@CNT nanoparticles, and DOX-loaded CS/PNIPAAm@CNT nanoparticles with NIR laser irradiation at pH 7.4. Data are presented as mean values ± SD (n = 6).

The thermal-sensitive and pH-dependent DOX release from the DOX-loaded CS/PNIPAAm@CNT nanoparticles was investigated by using dynamic dialysis. At predetermined intervals, 10 ml immersion solution was taken out from 50 ml dialysis solution and 10 ml fresh buffer solution was supplied to restore the volume to 50 ml. The solutions taken out at different time intervals were characterized by UV–vis spectrometry at 480 nm, which is the characteristic maximum absorbance of DOX in aqueous solution. Fig. 4A, shows the cumulative release profiles of DOX-loaded CS/PNIPAAm@CNT nanoparticles at various temperatures (25 °C and 40 °C) or various pH values (5.0 and 7.4). There was a slow release of about 10% of the incorporated DOX within 72 h in PBS at pH 7.4, 25 °C. When the pH value of the solution was dropped to 5.0 at 25 °C, the DOX release from nanoparticles was distinctly boosted, in which as high as above 30% of DOX was released in 72 h. As expected, the rate of DOX release from CS/PNIPAAm@CNT nanoparticles at 40 °C was accelerated in comparison with that at 25 °C, with ~12% release in the first 12 h and up to 27% release in 72 h. When the temperature was set at 40 °C while the pH was dropped to 5.0, the fastest drug release behavior was observed. Approximately 17% of DOX was released in the first 3 h and up to 40% DOX was continuously released in 72 h.

Considering the serum components are known to alter the properties of the nanovesicles, the characterization of the DOX release profile of nanoparticles in serum was conducted. As seen in Fig. 4B, it is difficult to tell the distinct difference when the nanoparticles were dispersed in buffer and in serum. However, it is found that impact of temperature on the drug release of nanoparticles was attenuated in serum in comparison with that in buffer. The exact reason is unclear in this study, which is believed to be relevant to the protein binding on the surface of the nanoparticles.

In the present research, NIR light irradiation will be used as a trigger to enhance the drug release from the DOX/CS-PNIPAAm@CNTs nanoparticles. As shown in Fig. 4A, there was a slow release of about 27% of the incorporated DOX within 72 h in PBS at pH 7.4, 40 °C. While the sample was irradiated by near-infrared light faculae for only 30 s, the release of DOX from the CS/PNIPAAm@CNT nanoparticles was greatly enhanced upon such stimulus. In a recent study of similar design, the chitosan-modified reduced graphene oxide incorporated into a thermosensitive nanogel (CGN) published by Wang et al. [45], it was found that a relative slower drug release was reported in this drug delivery system in

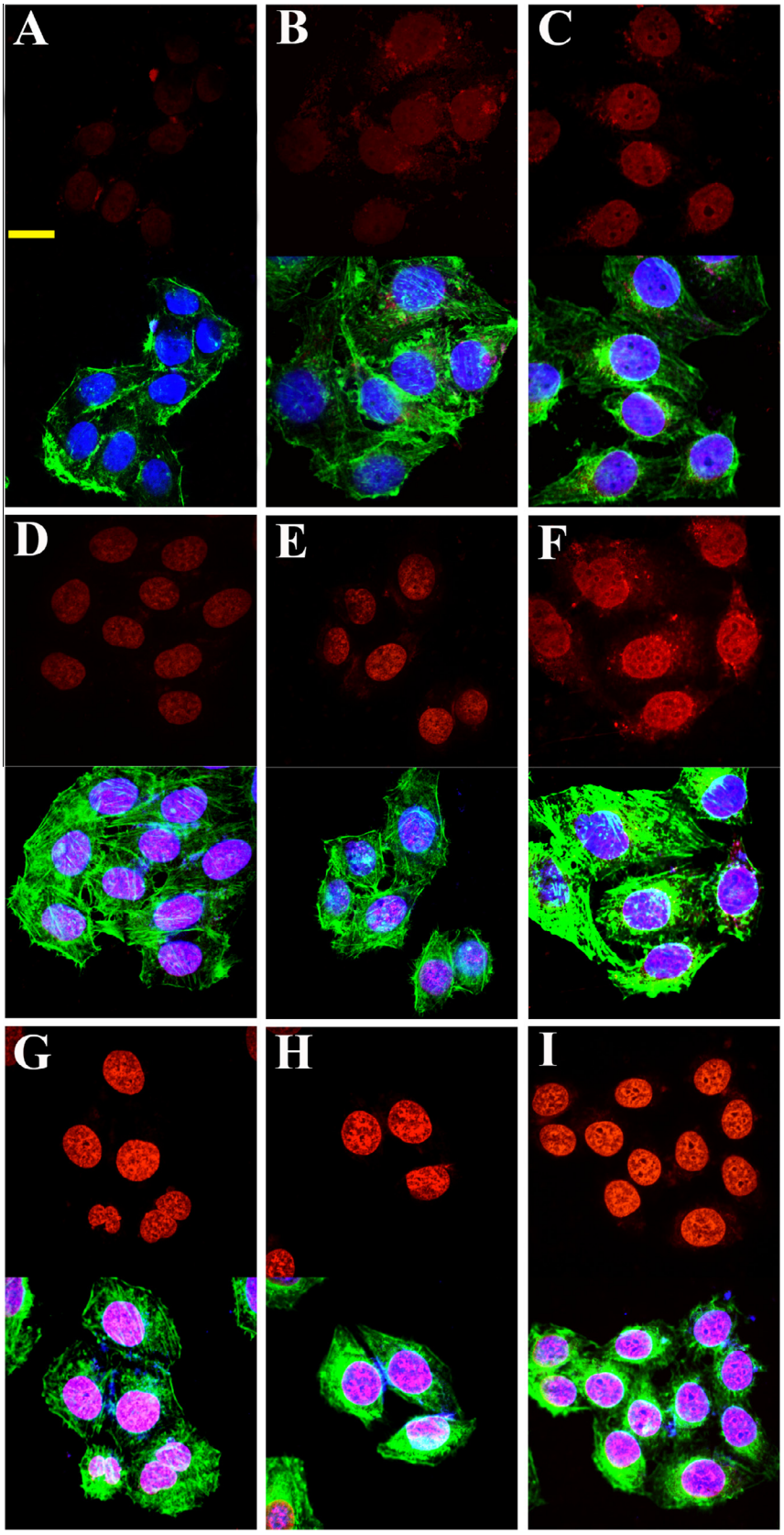

Fig. 6. Confocal laser scanning microscopy images of HeLa cells incubated with free DOX (A, D, G), DOX-loaded nanoparticles (B, E, H), DOX-loaded nanoparticles with NIR irradiation (C, F, I) for 15 min (A–C), 2 h (D–F) and 24 h (G–I). The upper row is the images of DOX distribution in the cells. The lower row is the merge images of nuclei (blue), F-actin (green) and DOX (red). The scale bar in A represents 15 μm.

Table 1
Quantitative fluorescence intensity of doxorubicin in the images presenting in Fig. 6 was obtained using the Image J software.

Sample	Area (Pixels)	Intensity	Intensity/pixel
A (Free DOX 15 min)	99181	2175.416	0.021933798
D (Free DOX 2 h)	169489	7982.751	0.047098933
G (Free DOX 24 h)	97707	12503.789	0.127972295
B (DOX-NPs 15 min)	194918	9234.689	0.047377302
E (DOX-NPs 2 h)	83810	6131.992	0.073165398
H (DOX-NPs 24 h)	62904	8573.748	0.136298932
C (DOX-NPs + NIR 15 min)	169617	8241.122	0.048586651
F (DOX-NPs + NIR 2 h)	197610	16802.914	0.085030687
I (DOX-NPs + NIR 24 h)	165053	22724.505	0.137680048

comparison with that of nanocomposites presenting in this work despite the fact that the drug loading content of CGN was as high as 48%. These results suggested that the strategy presenting in this work of nanovectors integrating CNT as a NIR antenna with pH/thermo-sensors can efficiently facilitate the drug release in a controllable fashion.

3.3. Cytotoxicity of DOX-loaded CS/PNIPAAm@CNT nanoparticles

To examine the biocompatibility or anti-cancer effects of the nanoparticles, HeLa cells were used to measure the inhibition rate of cell growth by using MTT assay. To this end, cells were exposed to different doses of free DOX, DOX-loaded CS/PNIPAAm@CNT or CS/PNIPAAm@CNT nanoparticles. As shown in Fig. 5, CS/PNIPAAm@CNT nanoparticles showed minimal cytotoxicity in the concentration range of 3–100 μg/ml, which indicated that the crosslinking procedure and chemical composition of the nanoparticles such as chitosan and PNIPAAm would not cause cytotoxicity. These results are in agreement with the previous reports [44,45]. The half inhibitory concentration (IC50) for free DOX is ~13 μg/ml and the equivalent IC50 DOX concentration for DOX-loaded CS/PNIPAAm@CNT nanoparticles at pH 7.4 is ~50 μg/ml. The cell growth inhibition rate of DOX-loaded CS/PNIPAAm@CNT nanoparticles was much lower than that of free DOX, due to the fact that DOX is much smaller and therefore can penetrate the cells relatively easier than DOX-loaded CS/PNIPAAm@CNT nanoparticles [33,46–48]. Thus, the less cytotoxicity for DOX-loaded CS/PNIPAAm@CNT without NIR irradiation conformed the function of the polymeric matrix in reserving DOX, being well consistent with the results of the recent research about the gold nanocage coated with a PNIPAAm corona published by Yang et al. [49]. After NIR laser irradiation (λ = 808 nm, 1 W/cm^2) for 10 min, DOX-CS/PNIPAAm@CNTs showed notably enhanced cell killing effects. For example, there was ~65% cell growth inhibition induced by NIR at the equivalent DOX concentration of 12 mg/ml, in comparison with ~20% cell growth inhibition without NIR irradiation. Combined with the results aforementioned in Fig. 4C, this significantly enhanced cell growth inhibition was attributed to the effective NIR light-triggered drug release, which was accomplished based on the thermal responsive drug release feature of our designed nanocomposites by virtue of high-efficient NIR light-heat conversion property of CNTs. The results were in accordance with the previous works of nanocomposites based on the CNTs or graphene oxide nanosheets, which promoted the diffusion of DOX and provided the photothermal treatment [45,50,51].

3.4. Enhanced cell uptake and intracellular drug distribution upon external stimuli

Confocal laser scanning microscopy (CLSM) was utilized to evaluate the cellular uptake and sequential intracellular drug distribution of DOX in HeLa cells. The cells were cultured in the cover slips at a density of 2 × 10^5 cells/slip (diameter = 24 mm) in the 6 well plates for 24 h. Then, the HeLa cells were exposed to free DOX and DOX-loaded CS/PNIPAAm@CNT nanoparticles with or without NIR irradiation.

As shown in Fig. 6, after 15 min incubation, the free DOX was visibly distributed in both the cytoplasm and the nuclei of the HeLa cells. Remarkably, after only 15 min of incubation with the DOX-loaded CS/PNIPAAm@CNT nanoparticles, DOX fluorescence was also observed in both cell cytoplasm and nuclei. After 2 h, stronger DOX fluorescence appeared in or around the nuclei, which indicated DOX was released from the nanoparticles and entered the cell nuclei.

To evaluate the enhanced cell internalization and NIR-induced DOX release from the CS/PNIPAAm@CNT nanoparticles, HeLa cells were irradiated by NIR laser for 1 min in every 15 min. After immunostaining of the fixed HeLa cells, the intracellular drug distribution was visualized by using CLSMs and the quantitative intensity of DOX intracellular was evaluated by the Image J software. As shown in Fig. 6, after NIR irradiation, more DOX fluorescence was found in nuclei and cytoplasm of HeLa cells than untreated control at pH 7.4. The intensity of DOX fluorescence was apparently increased with extended incubation (2 h, 24 h) and more NIR irradiation. It indicated that the NIR light can efficiently trigger the release of drugs from nanoparticles. After 24 h coculture with the nanoparticles or DOX, the intensity of DOX fluorescence from NIR-treated nanoparticles (~0.138 intensity/pixel) was higher than that from free DOX (~0.128 intensity/pixel) (see Table 1), suggesting an efficient release of DOX from these nanoparticles. The released DOX was concentrated in the nuclei and the cytoplasm area was shrunk which may be associated with cell inhibition induced by DOX. This phenomenon was in accordance with the other reports. At the same time, as typically shown in Fig. 6, more red fluorescent dots were observed in the cytoplasm regions when the cells were cocultured with the DOX-CS/PNIPAAm@CNT nanoparticles upon NIR irradiations in comparison with the cells treated with CS/PNIPAAm@CNT without NIR irradiations. Those red fluorescent dots were believed to be the nanoparticles encapsulating the drugs or its aggregations. This result suggested that more CS/PNIPAAm@CNT nanoparticles were taken up by the cells and stayed in the cytoplasm by virtue of NIR irradiations, which would be a key advantage of our strategy being able to facilitate the intracellular drug delivery. The reason for such enhanced cell internalization was unclear and still under study, but we hypothesized that the size variation and the temperature elevation of the nanoparticles played important roles in the whole process, for example the faster endocytosis caused by the size shrink, and faster endosomal escape partially attributed to the higher temperature, etc. Taken together, these results indicated that NIR can enhance the cell uptake of the CS/PNIPAAm @CNT nanoparticles and significantly enhance DOX release from nanovectors in cellular system.

4. Conclusions

In this report, a NIR sensitive CS/PNIPAAm@CNT nanoparticle was synthesized for the intracellular delivery of DOX. A simple and mild synthesis route was developed in this report to prepare the nanocomposite with good aqueous dispersion and narrow size distribution. The *in vitro* release of the entrapped DOX molecules from the nanoparticles was enhanced by changing temperature or pH, and more significantly by NIR irradiation. MTT assays showed the minimal cytotoxicity of as prepared CS/PNIPAAm@CNT nanoparticles and significantly enhanced cell killing behavior upon NIR laser irradiations. CLSM images indicated that CS/PNIPAAm@CNT nanoparticles could be employed as efficient NIR light triggered drug delivery nanovectors. These results highlighted the great potential of NIR-controlled drug release for targeted chemotherapy.

Acknowledgements

The authors gratefully acknowledge the National Natural Science Foundation of China (Grant No. 21304098, 21390411), National Basic Research Program of China (Grant No. 2011CB933101).

Appendix A. Figures with essential color discrimination

Certain figures in this article, particularly Figs. 1–6 are difficult to interpret in black and white. The full color images can be found in the on-line version, at http://dx.doi.org/10.1016/j.actbio.2015.01.026.

References

[1] Giri S, Trewyn BG, Stellmaker MP, Lin VSY. Stimuli-responsive controlled-release delivery system based on mesoporous silica nanorods capped with magnetic nanoparticles. Angew Chem Int Ed 2005;44:5038–44.
[2] Ganta S, Devalapally H, Shahiwala A, Amiji M. A review of stimuli-responsive nanocarriers for drug and gene delivery. J Control Release 2008;126:187–204.
[3] Schmaljohann D. Thermo- and pH-responsive polymers in drug delivery. Adv Drug Deliv Rev 2006;58:1655–70.
[4] Gil ES, Hudson SM. Stimuli-responsive polymers and their bioconjugates. Prog Polym Sci 2004;29:1173–222.
[5] Lai CY, Trewyn BG, Jeftinija DM, Jeftinija K, Xu S, Jeftinija S, et al. A mesoporous silica nanosphere-based carrier system with chemically removable CdS nanoparticle caps for stimuli-responsive controlled release of neurotransmitters and drug molecules. J Am Chem Soc 2003;125:4451–9.
[6] Alarcon CDH, Pennadam S, Alexander C. Stimuli responsive polymers for biomedical applications. Chem Soc Rev 2005;34:276–85.
[7] Stuart MAC, Huck WTS, Genzer J, Mueller M, Ober C, Stamm M, et al. Emerging applications of stimuli-responsive polymer materials. Nat Mater 2010;9:101–13.
[8] Zhu YF, Shi JL, Shen WH, Dong XP, Feng JW, Ruan ML, et al. Stimuli-responsive controlled drug release from a hollow mesoporous silica sphere/polyelectrolyte multilayer core-shell structure. Angew Chem Int Ed 2005;44:5083–7.
[9] Ariga K, Kawakami K, Hill JP. Emerging pressure-release materials for drug delivery. Expert Opin Drug Deliv 2013;10:1465–9.
[10] Kam NWS, O'Connell M, Wisdom JA, Dai HJ. Carbon nanotubes as multifunctional biological transporters and near-infrared agents for selective cancer cell destruction. Proc Natl Acad Sci USA 2005;102:11600–5.
[11] Timko BP, Dvir T, Kohane DS. Remotely triggerable drug delivery systems. Adv Mater 2010;22:4925–43.
[12] Wu G, Milkhailovsky A, Khant HA, Fu C, Chiu W, Zasadzinski JA. Remotely triggered liposome release by near-infrared light absorption via hollow gold nanoshells. J Am Chem Soc 2008;130:8175–7.
[13] You J, Zhang G, Li C. Exceptionally high payload of doxorubicin in hollow gold nanospheres for near-infrared light-triggered drug release. ACS Nano 2010;4:1033–41.
[14] Zhang Z, Wang J, Nie X, Wen T, Ji Y, Wu X, et al. Near infrared laser-induced targeted cancer therapy using thermoresponsive polymer encapsulated gold nanorods. J Am Chem Soc 2014;136:7317–26.
[15] Yang X, Liu X, Liu Z, Pu F, Ren J, Qu X. Near-infrared light-triggered, targeted drug delivery to cancer cells by aptamer gated nanovehicles. Adv Mater 2012;24:2890–5.
[16] Zhou L, Chen Z, Dong K, Yin M, Ren J, Qu X. DNA-mediated construction of hollow upconversion nanoparticles for protein harvesting and near-infrared light triggered release. Adv Mater 2014;26:2424–30.
[17] Ju E, Li Z, Liu Z, Ren J, Qu X. Near-infrared light-triggered drug-delivery vehicle for mitochondria-targeted chemo-photothermal therapy. ACS Appl Mater Interfaces 2014;6:4364–70.
[18] Niu N, He F, Ma P, Gai S, Yang G, Qu F, et al. Up-conversion nanoparticle assembled mesoporous silica composites: synthesis, plasmon-enhanced luminescence, and near-infrared light triggered drug release. ACS Appl Mater Interfaces 2014;6:3250–62.
[19] Kostarelos K, Bianco A, Prato M. Promises, facts and challenges for carbon nanotubes in imaging and therapeutics. Nat Nanotechnol 2009;4:627–33.
[20] Liu Z, Chen K, Davis C, Sherlock S, Cao Q, Chen X, et al. Drug delivery with carbon nanotubes for in vivo cancer treatment. Cancer Res 2008;68:6652–60.
[21] Nakanishi W, Minami K, Shrestha LK, Ji Q, Hill JP, Ariga K. Bioactive nanocarbon assemblies: nanoarchitectonics and applications. Nano Today 2014;9:378–94.
[22] Liu R, Zhao X, Wu T, Feng P. Tunable redox-responsive hybrid nanogated ensembles. J Am Chem Soc 2008;130:14418–9.
[23] Pantarotto D, Singh R, McCarthy D, Erhardt M, Briand JP, Prato M, et al. Functionalized carbon nanotubes for plasmid DNA gene delivery. Angew Chem Int Ed 2004;43:5242–6.
[24] Zhao M-Q, Zhang Q, Huang J-Q, Wei F. Hierarchical nanocomposites derived from nanocarbons and layered double hydroxides – properties, synthesis, and applications. Adv Funct Mater 2012;22:675–94.
[25] Ren J, Shen S, Wang D, Xi Z, Guo L, Pang Z, et al. The targeted delivery of anticancer drugs to brain glioma by PEGylated oxidized multi-walled carbon nanotubes modified with angiopep-2. Biomaterials 2012;33:3324–33.
[26] Wei H, Cheng S-X, Zhang X-Z, Zhuo R-X. Thermo-sensitive polymeric micelles based on poly(N-isopropylacrylamide) as drug carriers. Prog Polym Sci 2009;34:893–910.
[27] Zhang MG, Smith A, Gorski W. Carbon nanotube-chitosan system for electrochemical sensing based on dehydrogenase enzymes. Anal Chem 2004;76:5045–50.
[28] Bae Y, Fukushima S, Harada A, Kataoka K. Design of environment-sensitive supramolecular assemblies for intracellular drug delivery: polymeric micelles that are responsive to intracellular pH change. Angew Chem Int Ed 2003;42:4640–3.
[29] Prabaharan M, Grailer JJ, Pilla S, Steeber DA, Gong S. Amphiphilic multi-arm-block copolymer conjugated with doxorubicin via pH-sensitive hydrazone bond for tumor-targeted drug delivery. Biomaterials 2009;30:5757–66.
[30] Liu S, Ko ACT, Li W, Zhong W, Xing M. NIR initiated and pH sensitive single-wall carbon nanotubes for doxorubicin intracellular delivery. J Mater Chem B 2014;2:1125–35.
[31] Tan H, Chu CR, Payne KA, Marra KG. Injectable in situ forming biodegradable chitosan-hyaluronic acid based hydrogels for cartilage tissue engineering. Biomaterials 2009;30:2499–506.
[32] Wang Y, Zhou K, Huang G, Hensley C, Huang X, Ma X, et al. A nanoparticle-based strategy for the imaging of a broad range of tumours by nonlinear amplification of microenvironment signals. Nat Mater 2014;13:204–12.
[33] Chen J, Qiu X, Ouyang J, Kong J, Zhong W, Xing MMQ. PH and reduction dual-sensitive copolymeric micelles for intracellular doxorubicin delivery. Biomacromolecules 2011;12:3601–11.
[34] Huang C-H, Wang C-F, Don T-M, Chiu W-Y. Preparation of pH- and thermo-sensitive chitosan-PNIPAAm core–shell nanoparticles and evaluation as drug carriers. Cellulose 2013;20:1791–805.
[35] Duan C, Gao J, Zhang D, Jia L, Liu Y, Zheng D, et al. Galactose-decorated pH-responsive nanogels for hepatoma-targeted delivery of oridonin. Biomacromolecules 2011;12:4335–43.
[36] Kono K, Kojima C, Hayashi N, Nishisaka E, Kiura K, Wataral S, et al. Preparation and cytotoxic activity of poly(ethylene glycol)-modified poly(amidoamine) dendrimers bearing adriamycin. Biomaterials 2008;29:1664–75.
[37] Heister E, Neves V, Lamprecht C, Silva SRP, Coley HM, McFadden J. Drug loading, dispersion stability, and therapeutic efficacy in targeted drug delivery with carbon nanotubes. Carbon 2012;50:622–32.
[38] Mehra NK, Verma AK, Mishra PR, Jain NK. The cancer targeting potential of D-alpha-tocopheryl polyethylene glycol 1000 succinate tethered multi walled carbon nanotubes. Biomaterials 2014;35:4573–88.
[39] Chuang C-Y, Don T-M, Chiu W-Y. Synthesis and properties of chitosan-based thermo- and pH-responsive nanoparticles and application in drug release. J Polym Sci A: Polym Chem 2009;47:2798–810.
[40] Lee ES, Na K, Bae YH. Super pH-sensitive multifunctional polymeric micelle. Nano Lett 2005;5:325–9.
[41] Bae Y, Nishiyama N, Fukushima S, Koyama H, Yasuhiro M, Kataoka K. Preparation and biological characterization of polymeric micelle drug carriers with intracellular pH-triggered drug release property: tumor permeability, controlled subcellular drug distribution, and enhanced in vivo antitumor efficacy. Bioconjug Chem 2005;16:122–30.
[42] Meng H, Liong M, Xia T, Li Z, Ji Z, Zink IJ, et al. Engineered design of mesoporous silica nanoparticles to deliver doxorubicin and P-glycoprotein siRNA to overcome drug resistance in a cancer cell line. ACS Nano 2010;4:4539–50.
[43] Oh JK, Siegwart DJ, Lee HI, Sherwood G, Peteanu L, Hollinger JO, et al. Biodegradable nanogels prepared by atom transfer radical polymerization as potential drug delivery carriers: synthesis, biodegradation, in vitro release, and bioconjugation. J Am Chem Soc 2007;129:5939–45.
[44] Gui R, Wang Y, Sun J. Embedding fluorescent mesoporous silica nanoparticles into biocompatible nanogels for tumor cell imaging and thermo/pH-sensitive in vitro drug release. Colloids Surf B: Biointerfaces 2014;116:518–25.
[45] Wang C, Mallela J, Garapati US, Ravi S, Chinnasamy V, Girard Y, et al. A chitosan-modified graphene nanogel for noninvasive controlled drug release. Nanomed. NBM 2013;9:903–11.
[46] Chen J, Zehtabi F, Ouyang J, Kong J, Zhong W, Xing MMQ. Reducible self-assembled micelles for enhanced intracellular delivery of doxorubicin. J Mater Chem 2012;22:7121–9.
[47] Bareford LA, Swaan PW. Endocytic mechanisms for targeted drug delivery. Adv Drug Deliv Rev 2007;59:748–58.
[48] Mukherjee S, Ghosh RN, Maxfield FR. Endocytosis. Physiol Rev 1997;77:759–803.
[49] Yang J, Shen D, Zhou L, Li W, Li X, Yao C, et al. Spatially confined fabrication of core–shell gold Nanocages@Mesoporous silica for near-infrared controlled photothermal drug release. Chem Mater 2013;25:3030–7.
[50] Wan H, Zhang Y, Liu Z, Xu G, Huang G, Ji Y, et al. Facile fabrication of a near-infrared responsive nanocarrier for spatiotemporally controlled chemo-photothermal synergistic cancer therapy. Nanoscale 2014;6:8743–53.
[51] Song E, Han W, Li C, Cheng D, Li L, Liu L, et al. Hyaluronic acid-decorated graphene oxide nanohybrids as nanocarriers for targeted and pH-responsive anticancer drug delivery. ACS Appl Mater Interfaces 2014;6:11882–90.